Chemical Engineering Journal 95 (2003) 235–240

Chemical Engineering Journal

www.elsevier.com/locate/cej

# Numerical simulation of the effects of turbulence intensity and boundary layer on separation efficiency in a cyclone separator

Li Xiaodong*, Yan Jianhua, Cao Yuchun, Ni Mingjiang, Cen Kefa

*Institute for Thermal Power Engineering, Zhejiang University, Clean Energy and Environmental Engineering, Key Laboratory of Ministry Education, Hangzhou 310027, PR China*

**Abstract**

From the point of view of the influence of turbulence structure, this paper presents an elementary numerical analysis of the interaction between a particle and a gas phase. The effects of turbulence structure and the thickness of boundary layer on the separation efficiency in a cyclone separator have been investigated. The effects of the Saffman force on the particle trajectory are also analyzed. The results indicate that the separation efficiency decreases with an increase in turbulence intensity and increases with a decrease in the thickness of the boundary layer. The Saffman force can enhance the separation of small particles and also can shorten their residence time in the cyclone.


*Keywords:* Two-phase flow; Separation; Turbulence intensity; Boundary layer

## 1. Introduction

The techniques of gas–solid separation are extensively applied in the energy and chemical industries. The cyclone separator is a typical gas–solid separator. Various researchers have already made detailed studies on the effects of a solid phase on gas phase velocity profiles in a cyclone. Most of them found under conditions of high particle concentration the separation efficiency always decreased with increased particle concentration [1,2]. Tuzla and Chen [3] considered that there was a maximum particle concentration below which the separation efficiency increased and above which it decreased. Betal [4] considered that an agglomeration effect resulting from turbulence was very obvious because the turbulence intensity in a cyclone separator was very strong. Bloor and Iagham [5] studied the effect of a particle phase on the flow with a similar fluid model. Their conclusions gave a good explanation of why the separation efficiency would increase under conditions of high particle concentration with an increment in tangential velocity because of the existence of the solid phase, and also decrease with an increment in the thickness in the condensed zone of particles near the wall surface of the separator. But, they only investigated the influence of the particle phase on the mean flow fields, not on the turbulence structure. Peskin [6] did a study on the interaction of the gas and solid phases in the turbulence, and found that particles with small diameter (about $<0.5$ mm) could weaken turbulent fluctuations in the gas phase. In their study of the effect of the particle phase on the turbulence structure in the isotropic turbulence, Squires and Eaton [7] found that the particles phase not only enhanced the high frequency parts of the turbulence, but also reduced the low frequency parts and lessened the turbulent energy dissipation, i.e. reduced the resistance loss.

In order to further study the effect of turbulence intensity on separation efficiency, a numerical analysis has been done. Considering a typical cyclone as the research object, this numerical simulation focuses on two important factors: the effects of turbulence intensity and the thickness of the boundary layer on the separation efficiency. As there are velocity gradients in the flow fields, the particles will have imposed on them a lifting force named the Saffman force due to the effects of fluid shear. In this paper, calculations for the effects of the Saffman force on the boundary layer are also considered.

## 2. Multi-phase gas–solid flow model

Fig. 1 shows a schematic of a cyclone. Zhou and Soo's [8] analysis was adapted to determine the gas-phase velocity field in the cyclone. Liu et al.'s test data [9] were taken as reference. In the process of determining the particle trajectory, two assumptions were made as follows:

* Corresponding author. Tel.: +86-571-8795-1294; fax: +86-571-8795-2438.
*E-mail address:* lixd@cmee.zju.edu.cn (L. Xiaodong).

1385-8947/$ – see front matter 
doi:10.1016/S1385-8947(03)00109-8

**Nomenclature**

| | |
|---|---|
| $C$ | the maximum vorticity |
| $C_D$ | drag coefficient |
| $d$ | diameter of cyclone |
| $D_0$ | diameter of the main section of the cyclone |
| $D_1$ | diameter of the gas exit throat of the cyclone |
| $D_2$ | diameter of the particle exit throat of the cyclone |
| $f_b$ | main fluctuation frequency |
| $I$ | turbulence intensity, 1–3 |
| $L$ | height of the cyclone |
| $Q$ | flow rate of the gas |
| $r$ | radius |
| $R$ | radius of the cyclone |
| $Re$ | Reynolds number based on length and velocity |
| $u$ | radial velocity component |
| $v$ | tangential velocity component |
| $v_B$ | velocity on the edge of the boundary layer |
| $v_{in}$ | inlet velocity of the cyclone |
| $v_T$ | the maximum tangential velocity |
| $w$ | axial velocity component |
| $\bar{w}$ | mean axial velocity of the cyclone |
| $w_0$ | mean outlet velocity of the cyclone |
| $z$ | height |
| $Z_o$ | height of the upper section of the cyclone |
| $Z_e$ | height of the lower section of the cyclone |

*Greek symbols*

| | |
|---|---|
| $\delta$ | thickness of the boundary layer viscosity |
| $\mu$ | viscosity |
| $\rho$ | density |

*Subscripts*

| | |
|---|---|
| g | gas phase |
| p | solid phase |

(1) The forces affecting the particles include only gravity, drag force, centrifugal force and the force resulting from the velocity gradient (the Saffman force).
(2) Regardless of the interaction among the particles, the interaction between the particles and the wall surface is taken into consideration.

### 2.1. Mean velocity field of the gas phase

#### 2.1.1. Tangential velocity

When $z < (L - S)$, Zhou and Soo's analytical solution [8] is adapted:

$$v = \frac{C}{r}\left[1 - \exp\left(-\frac{r^2}{R_C^2}\right)\right] \qquad (1)$$

where $C$ is the maximum velocity and $R_C$ the radius of the core of solid body rotation [8].

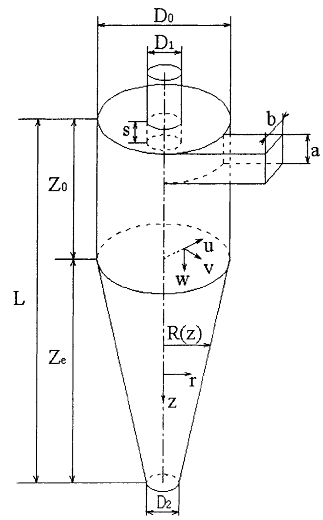


Fig. 1. The schematic of the cyclone.

When $z \geq (L - S)$, the tangential velocity distribution is parabolic and is close to zero on the outside surface of the exit pipe. The maximum tangential velocity occurs where $r = (2D_0 + D_1)/6$ and approximately coincides with Eq. (1). So, the maximum tangential velocity $v_T$ also can be determined by Eq. (1) and then:

$$v = v_T\left[1 - \frac{(r - ((2D_0 + D_1)/6))^2}{((D_0 + D_1)/3)^2}\right] \qquad (2)$$

#### 2.1.2. Axial velocity

When $z < (L - S)$, Zhou and Soo's analysis solution [8] is adapted:

$$w = \bar{w} \cdot Z^{**} \cdot f(r^{**}) \qquad (3)$$

In Eq. (3),

$$Z^{**} = \begin{cases} z/Z_e, & z \leq Z_e \\ 1, & z > Z_e \end{cases},$$

$f(r^{**}) = a_0 + a_1 r^{**2} + a_1 r^{**4} + a_1 r^{**6}$, and $r^{**} = r/R(z)\cdot$

The $a_0$, $a_1$, and $a_2$ are constants. $R(z)$ is the radius of the cyclone according to the position where the particles locate.

When $z \geq (L - S)$, the axial velocity is given [9]:

$$w = \begin{cases} -1, & r \geq (2D_1 + D_0)/6 \\ -1 + \dfrac{90r'}{D_0 - D_1}, & r < (2D_1 + D_0)/6 \end{cases} \qquad (4)$$

where $r' = r - (2D_1 + D_0)/6$.

#### 2.1.3. Radial velocity

For the distribution of the radial velocity in the cyclone, the following equation is used [9]:

$$u = \begin{cases} -2, & r \geq R_C \\ -\dfrac{12r}{R_C} + 10, & R_C > r > \dfrac{5R_C}{12} \\ -\dfrac{12r}{R_C}, & \dfrac{5R_C}{12} > r \geq 0 \end{cases} \qquad (5)$$

*2.1.4. The distribution of the velocity in the boundary layer*

An assumption is made that the distribution of velocity in the boundary layer is parabolic. Taking the tangential velocity as an example, we suppose that the velocity at the edge of the boundary layer is $v_B$ according to Eqs. (1) and (2). So, the distribution of the tangential velocity in the boundary layer will be:

$$v = v_B \frac{[R(z) - r]^2}{\delta^2} \tag{6}$$

The radial velocity and the tangential velocities are also dealt with in such a way.

### 2.2. The fluctuation velocity in the gas phase

The instantaneous velocity of the gas flow consists of the time–mean velocity and the fluctuation velocity. A random Fourier series is used to simulate the gas velocity as follows:

$$u' = \sum^{n} R_1 u_{im} \cos(\mathrm{i} w_i t - R_2 a_i^u),$$
$$v' = \sum^{n} R_3 v_{im} \cos(\mathrm{i} w_i t - R_4 a_i^v),$$
$$w' = \sum^{n} R_5 w_{im} \cos(\mathrm{i} w_i t - R_6 a_i^w) \tag{7}$$

In Eq. (7), $u'$, $v'$ and $w'$ represent the velocities in the radial, tangential and axial directions, $R_1 \sim R_6$ are random numbers in terms of the normal distribution, $a_i^u$, $a_i^v$ and $a_i^w$ are the relative angles of the fluctuations, $u_{im}$ $v_{im}$ and $w_{im}$ are the scopes of the fluid eddy fluctuations with a certain frequency that are determined according to a concrete turbulent fluctuation. The fluctuation scopes of the fluid eddy are determined according to the existing results rooted in the experiments or calculation [8,9,10,11].

### 2.3. The equation of motion for the particles

In the three-dimensional cylindrical coordinates, for a particle, only gravity, drag force, centrifugal force and the force resulting from the velocity gradient (the Saffman force) are considered, the equation of motion is:

$$\frac{\mathrm{d}u_P}{\mathrm{d}t} = \frac{1}{\tau_r}(u + u' - u_P) + \frac{v_P^2}{r} - F_{saff},$$
$$\frac{\mathrm{d}v_P}{\mathrm{d}t} = \frac{1}{\tau_r}(v + v' - v_P) + \frac{u_P v_P}{r},$$
$$\frac{\mathrm{d}w_P}{\mathrm{d}t} = \frac{1}{\tau_r}(w + w' - w_P) - g \tag{8}$$

where $\tau_r$ is the relaxation time of the particle, $\tau_r = (\rho_P d_P^2)/(18\mu f)$ and $f = C_D/(24/Re)$. The drag coefficient in the turbulent fluctuation flow is:

$$C_D = \frac{24}{Re}(1 + 0.19Re^{0.62}) \left[1 + 0.095\left(\frac{f_b Re}{\sigma}\right)^{0.287}\right] \tag{9}$$

Here, $f_b$ is the main fluctuation frequency and $\sigma$ is a fitting constant of frequency spectrum, which is determined by experiment.

In Eq. (8), $F_{saff}$ is the Saffman force, which can be calculated as follow [12]:

$$F_{saff} = \frac{9.66}{\pi d_p}(\mu \rho g)^{1/2}(v_g - v_P)\left|\frac{\mathrm{d}v}{\mathrm{d}r}\right|^{1/2} \tag{10}$$

Here, $\mathrm{d}v/\mathrm{d}r$ is the gradient of the tangential velocity.

After calculating the velocity of the particle according to Eq. (8), we can determine the particle trajectory.

### 2.4. The turbulence intensity of the gas phase in a cyclone

Turbulence intensity can be calculated as follow [8,9,12]:

$$I = \begin{cases} I_1, & r > R(z) - \delta \\ I_2, & R(z) - \delta \geq r \geq R_c \\ I_2 + (I_3 - I_2)(R_c - r)/R_c, & \delta < R_c \end{cases} \tag{11}$$

In the normal condition, the turbulence intensities $I_1 = I_2 = 5\%$ and $I_3 = 30\%$. Different turbulence intensities and thickness of the boundary layer were used to study their effects on the cyclone's separation efficiency.

### 2.5. The relevant parameters calculation of the model

The inlet conditions adopted for the cyclone are given as follows: the inlet flow rate of gas $Q = 0.266\,\mathrm{m^3/s}$ the inlet velocity $v_{in} = 21\,\mathrm{m/s}$, the mean axial velocity $\bar{w} = 3.75\,\mathrm{m/s}$, and the mean velocity of outlet pipe (from the top pipe of the cyclone) $w_0 = 11.7\,\mathrm{m/s}$. The parameters of the cyclone are listed in the Table 1.

The referent thickness of the boundary layer is 5 mm [5]. The thickness in different conditions and $I_1$–$I_3$ are shown in Table 2.

In order to investigate residence time through the cyclone, particle groups with various diameter were selected. During the calculation, each group of 100 particles was uniformly put into the inlet section, thus we can consider that the mean residence time was: $\sum_{i=1}^{100} t_i/100$.

Table 1
The geometrical parameters of the cyclone separator

| Parameters | Values (m) |
|---|---|
| $D_0$ | 0.30 |
| $Z_o$ | 0.394 |
| $D_1$ | 0.17 |
| $D_2$ | 0.11 |
| $Z_e$ | 0.686 |
| $L$ | 1.08 |
| $a$ | 0.115 |
| $b$ | 0.11 |

Table 2
The relevant parameters for calculation in the different conditions

| | Item no. | | | | | | | | | | |
|---|---|---|---|---|---|---|---|---|---|---|---|
| | 1 | 2 | 3 | 4* | 5 | 6 | 7 | 8 | 9 | 10 | 11 |
| The thickness of the boundary layer (mm) | 5 | 5 | 5 | 5 | 5 | 5 | 1 | 3 | 7 | 9 | 11 |
| $I_1$ (%) | 0 | 2 | 3 | 5 | 6 | 7 | 5 | 5 | 5 | 5 | 5 |
| $I_2$ (%) | 0 | 3.5 | 4 | 5 | 7 | 9 | 5 | 5 | 5 | 5 | 5 |
| $I_3$ (%) | 0 | 15 | 22 | 30 | 40 | 50 | 30 | 30 | 30 | 30 | 30 |

*Note*: The * means the reference calculation condition.

## 3. Results and analysis

### 3.1. The effects of the velocity gradient force (the Saffman force)

Fig. 2 shows a comparison of the residence times when considering the effects of the velocity gradient force or not. Except for the smallest particles regardless of the effect of the Saffman force for the reason that they cannot reach the boundary layer, the residence time of the other particles without considering the Saffman force will be slightly increased, over those calculated in the absence of the Saffman force. The maximal deviation occurs for the 20 μm particles and reaches approximately 10 s.

Fig. 3 shows a comparison of the separation efficiencies when considering the Saffman force or not and indicates that the only obvious effects are on the particles ranging in diameter from 7.5 to 20 μm. As the particles below 7.5 μm cannot reach the boundary layer, the Saffman force has no effect on their separation efficiency. It also has no obvious effects on the particles with large diameter because they have a relatively larger inertia.

Fig. 4 shows the effect of the Saffman force on the particle trajectory: $r/R(z)$ and $I - z/L$, respectively, refer to the non-dimensional positions in the radial and axial directions. The place where the Saffman force has an obvious effect on the particles has been marked on the curves shown in Fig. 4. Through the comparison of the two curves we can see that the Saffman force accelerates the particles to move close to the surface of the wall, and at the same time, after reflecting from the wall, the particles have great fluctuation in their velocities. Tile particle trajectories have no difference with or without consideration of the Saffman force. So, we can draw a conclusion that accelerating the particles close to the wall surface enhances the separation of the particles.

The direction of the Saffman force depends on the relative velocity between the particle and the gas phase. When the velocity of the particle is less than that of the gas phase, the direction of the Saffman force will point towards the axis of the cyclone, whereas it will point to the surface of the wall if the particle velocity is greater than that of the gas phase. When the particles enter the boundary layer, and their tangential velocities are more than the local velocity of the gas phase, they will be accelerated toward the surface of the wall and their tangential velocities will be weakened. However, after rebounding from the surface, their tangential velocities may be less than the local velocity of the gas

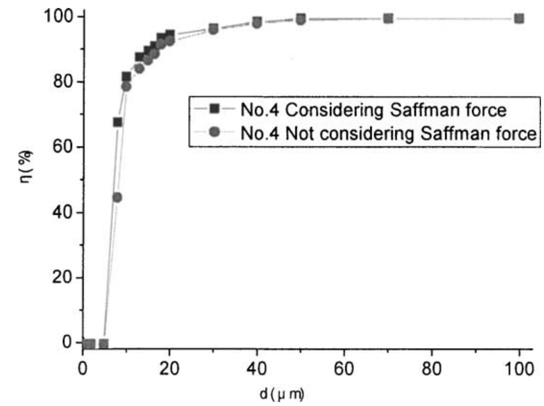


Fig. 3. The effect of the Saffman force on the separation efficiency.

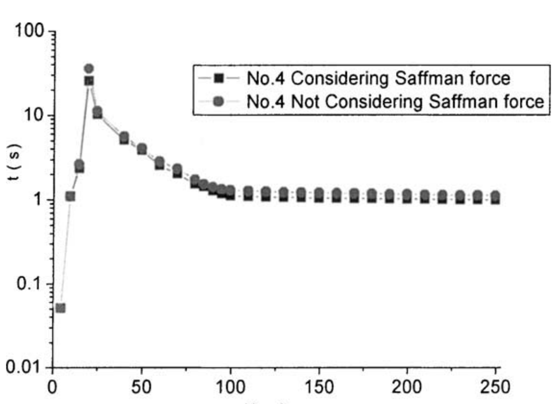


Fig. 2. The effect of the Saffman force on the residence time of the particles.

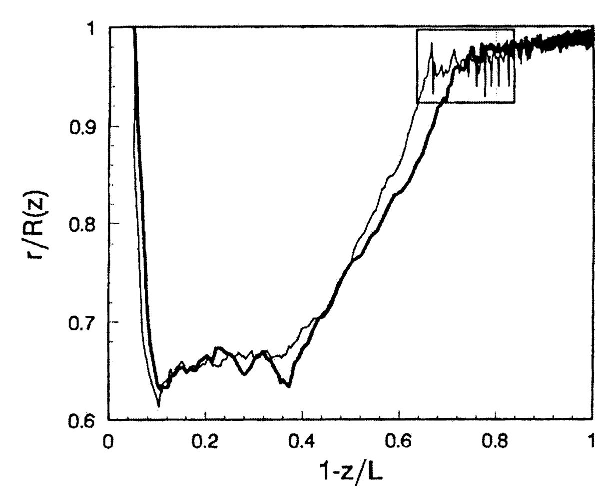


Fig. 4. The effect of the Saffman force on the particle trajectory ($d_P$ = 7.5 μm): (—) not considering Saffman force; (▬) considering Saffman force.

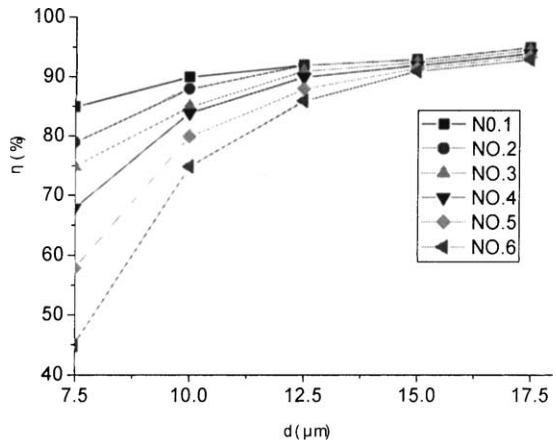


Fig. 5. The effect of turbulence intensity on the separation efficiency.

phase, and the Saffman force would tend to move them towards the axis. Thereafter their tangential velocity might be accelerated again and they would move toward the boundary layer with the effects of the centrifugal force. Through such repetitions of the process and acted on by the centrifugal force the drag force of the gas phase and the Saffman force, overall the particles move gradually toward the surface of the wall. During the fluctuation of the particles velocity, imposed mainly by the Saffman force, the turbulent fluctuation also has positive effects on the above process to some degree.

### 3.2. The effects of the turbulence intensity in the cyclone separator

Fig. 5 shows the effects of variations in turbulence intensity on the separation efficiency. Fig. 6 shows the effect of various turbulence intensities on the mean residence times of the particles. The symbols in the two figures represent different condition numbers (the actual value of turbulence intensity can be determined according to Table 2). Obviously, with increase in turbulence intensity the separation efficiency decreases when the particles are <17.5 μm. When the particles are more than 30 μm, the intensity has almost no effects on the residence time because the particles have relatively bigger inertias. But, for the particles <5 μm, the residence time decreases with increases in the turbulence intensity. For the particles from 5 to 30 μm, the residence time of relatively large particles will increase with the turbulence intensity, whereas that of relatively smaller particles will decrease. The reason is that with an increment in the turbulence intensity, the residence time of the separated particles will increase, but at the same time the turbulence intensity may take the separated particles into the main gas flow and the residence time would be sharply shortened. The residence time of the relatively large particles may be longer because an increment in the turbulence intensity has almost no effects on their separation efficiency, whereas for the relatively smaller particles, their mean residence time will be shortened because of the increment of the turbulence intensity. So, the effects of the turbulence intensity on the separator efficiency depend not only on the concentration of the particles, but also on their distribution of diameters.

Fig. 7 shows the effects of the various turbulence intensities on the particle trajectories. Obviously, the scope of the deviation from the mean trajectory (no. 4) will increase with increasing the turbulence intensity in the gas phase. Where $r/R(z)$ is relatively small, $1 - Z/L$ is between 0.1 and 0.4 as shown in the Fig. 7. Once the scope of deviation reaches a certain degree, the increment of the turbulent will make the particles enter the zone where the axial velocity of the gas phase is upward which gives a good explanation of why the separation efficiency of the relatively smaller particles decreases with increase in the turbulence intensity.

### 3.3. The effect of the thickness of the boundary layer

Fig. 8 indicates the effects of thickness of the boundary layer on the separation efficiency of the cyclone (the actual

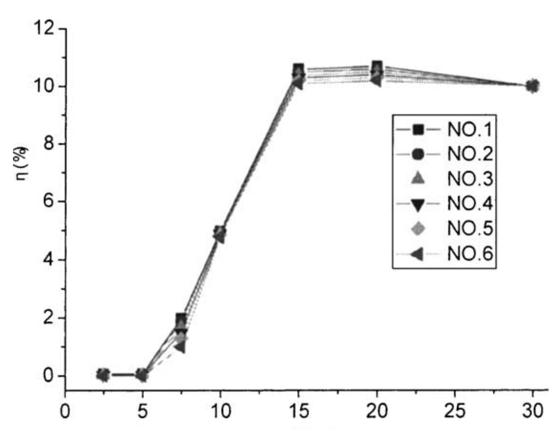


Fig. 6. The effect of turbulence intensity on the mean residence time.

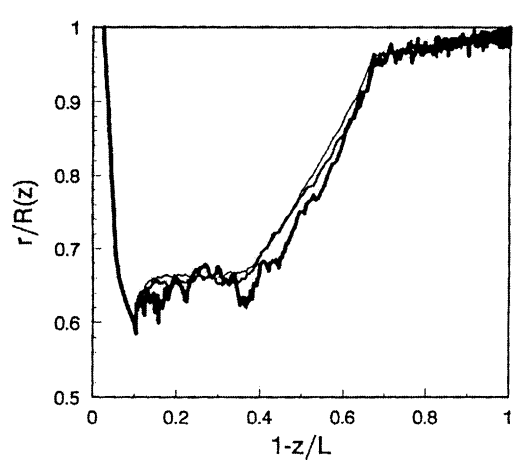


Fig. 7. The effect of turbulence intensity on the particle trajectory, $d_P = 7.5\,\mu m$: (—) no. 2; (▬▬) no. 4; (▬▬) no. 6.

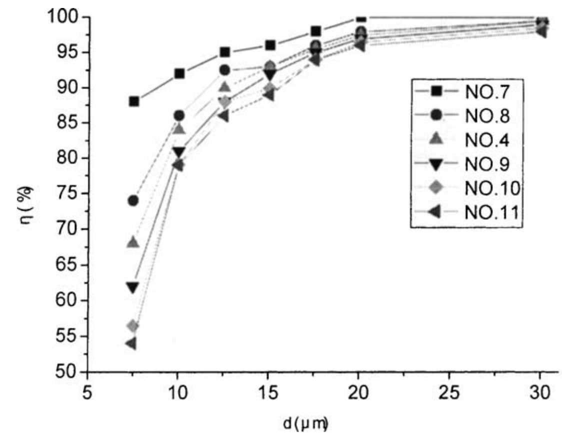


Fig. 8. The effects of the thickness of the boundary layer on the separation efficiency.

thickness of the boundary layer corresponding to various conditions can be found in Table 2). The results show that the efficiency increases with a decrease in the thickness of the boundary layer for the particles of diameter $<30\,\mu m$. As such a decrease means that the main flow zone with a large tangential velocity may be enlarged so that the area where there is a relatively strong centrifugal force on the particles, is enlarged so that the particles are more easily separated.

## 4. Conclusion

With the gas–solid flow model of the particles in a cyclone, we have studied the effects of turbulence intensity, thickness of the boundary layer and the Saffman force resulting from velocity gradient on the separation performance. The following conclusions are drawn from the results.

(1) The mean residence time of most of the particles is more than 1 s.
(2) The Saffman force can accelerate the separation of small particles; it can also shorten their residence time.
(3) With increased intensity of the turbulence, the separation efficiency of small particles will decrease. The effects of the increase on the mean residence time are much more complex. The effects of the intensity on the separation efficiency depend on not only the concentration but also on the particle size distribution characteristics.
(4) With a decrease in the thickness of the boundary layer, the separation efficiency will increase.

## References

[1] A.C. Hoffmann, An experimental investigation elucidating the nature of the effect of solids loading on cyclone performance, Filtr. Sep. 28 (May 1991) 188–193.
[2] M.E. Fayed, L. Otten, Handbook of Powder Science and Technology, Van Nostrand Reinhold Co., New York, 1984.
[3] K. Tuzla, J.C. Chen, Performance of a cyclone under high solid loadings, AICHE Symp. Ser. 88 (289) (1992) 130–138.
[4] W. Batel, Dust Extraction: Technology Principle, Methods, Measurement Technique, Stonehouse Technicopy, England, 1976.
[5] M.L.G. Bloor, D.B. Iagham, Theoretical aspects of hydrocyclone flow, in: R.J. Wakeman (Ed.), Progress in Filtration and Separation Part III, Elsevier, Amsterdam, 1983.
[6] R.L. Peskin, Turbulent fluid–particle interaction, in: G. Hetsronil (Ed.), Handbook of Multiphase System, Hemisphere Publishing Corporation, Washington DC, 1982.
[7] K.D. Squires, J.K. Eaton, Particle response and turbulence modification in isotropic turbulence, Phys. Fluids A2 (7) (1990) 1191–1203.
[8] L.X. Zhou, S.L. Soo, Gas–solid flow and collection of solids in a cyclone separator, Powder Technol. 63 (1990) 45–53.
[9] Q. Liu, J. Fu, Z. Dili, H. Jinrao, W. Pingsheng, X. Jihua, The measurement of a three-dimension flow field in the cyclone separator, J. Mech. 3 (1978) 182–191.
[10] S.L. Soo, Multiphase Fluid Dynamics, University of Illinois, Urbana, 1983.
[11] L.X. Zhou, Theory and Numerical Modeling of Turbulent Gas–Particle Flows and Combustion, Science Press/CRC Press Inc., Boca Raton, 1993.
[12] K. Cen, J. Fan, The Theory and Calculation of Engineering Multiple-Phase Flow, Zhejiang University Press, Hangzhou, China, 1990.